Supplement

Table S1. Value of Tb_{fit}, f_{NOx} and f_{PM} for each EU-27 country. The missing data for the calculation of $f_{spec.}$ have been replaced by the European average available (numbers underlined).

Country	Tb_{fit}	f_{NOx}	f_{PM}
Austria	15.92	0.12	0.07
Belgium	15.92	0.16	0.01
Bulgaria	15.65	0.19	0.04
Croatia	15.82	0.27	0.05
Cyprus	15.35	<u>0.25</u>	0.02
Czechia	15.58	0.35	0.04
Denmark	15.03	0.28	0.06
Estonia	12.49	0.27	0.12
Finland	11.99	0.22	0.24
France	15.96	0.17	0.04
Germany	15.45	0.21	0.07
Greece	15.60	0.13	0.01
Hungary	17.69	0.17	0.01
Ireland	15.39	0.29	0.12
Italy	15.68	0.25	0.04
Latvia	11.49	0.48	0.15
Lithuania	13.52	0.34	0.07
Luxembourg	15.67	0.12	0.02
Malta	15.57	<u>0.25</u>	0.01
Netherlands	15.43	0.23	0.01
Poland	15.10	0.47	0.10
Portugal	15.52	0.94	0.29
Romania	16.63	0.41	0.23
Slovakia	16.14	0.20	0.25
Slovenia	15.85	0.27	0.22
Spain	15.62	0.54	0.11
Sweden	11.99	0.24	0.11

Table S2. Characteristics of domestic gas data-sets from the ENTSOG Transparency platform. For each country, the gas supplier used and the period covered by the data are detailed.

Country	Gas supplier	Time cover
Hungary	FGSZ	2019-2021
Roumania	Transgas	2018-2021
Italy	Snam Rete Gas	2016-2021
France	GRTgas	2016-2021
Belgium	Fluxys Belgium	2016-2021
Netherlands	GTS	2016-2021
Latvia	Conexus	2020-2021
Estonia	Elering Gaas	2016-2021

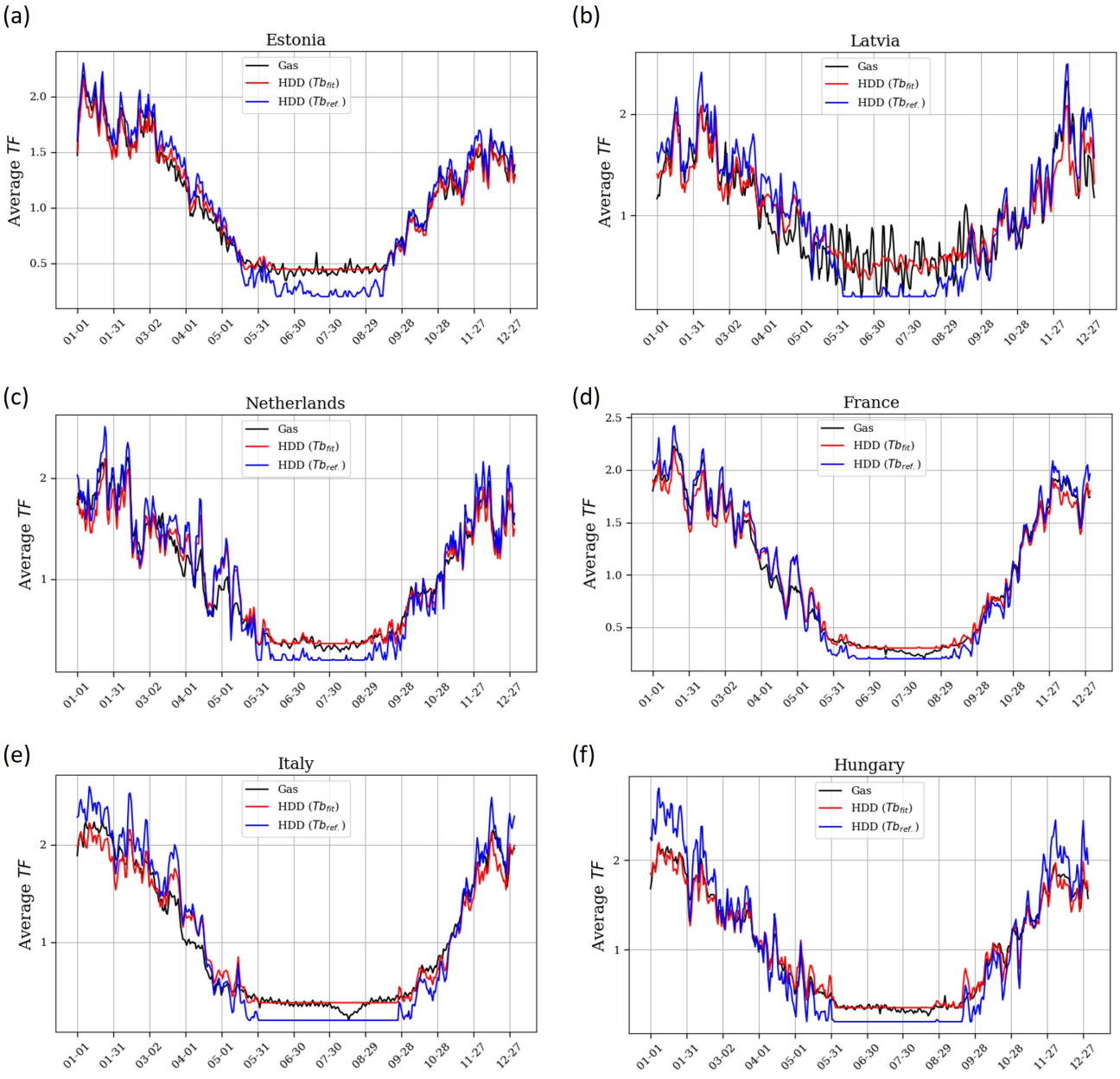

Figure S1. Daily evolution of $TF(c)$ (unitless) for gas consumption (in black), for HDDs with Tb_{fit} (in red) and for HDDs with $Tb_{ref.}$ (in blue). $TF(c)$ is averaged over the period 2018-2021 for Estonia (a), over 2020-2021 for Latvia (b), over 2016-2021 for Netherlands (c), over 2016-2021 for France (d), over 2016-2021 for Italy (e) and over 2019-2021 for Hungary (f).

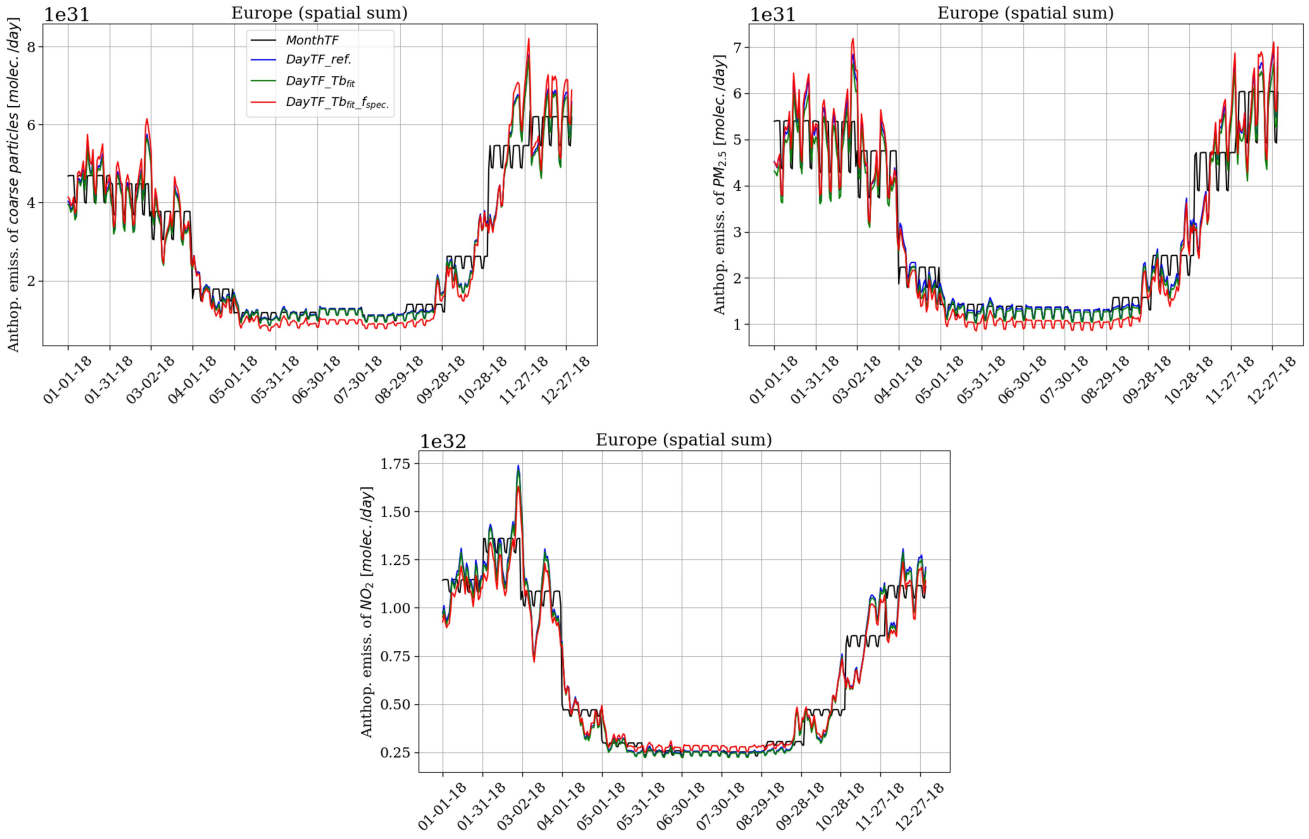

Figure S2. Time series at daily time step of total anthropogenic emissions of coarse particles (top left), fine particles (top right) and NO_2 (bottom) in Europe for the different experiments detailed in Table 2.

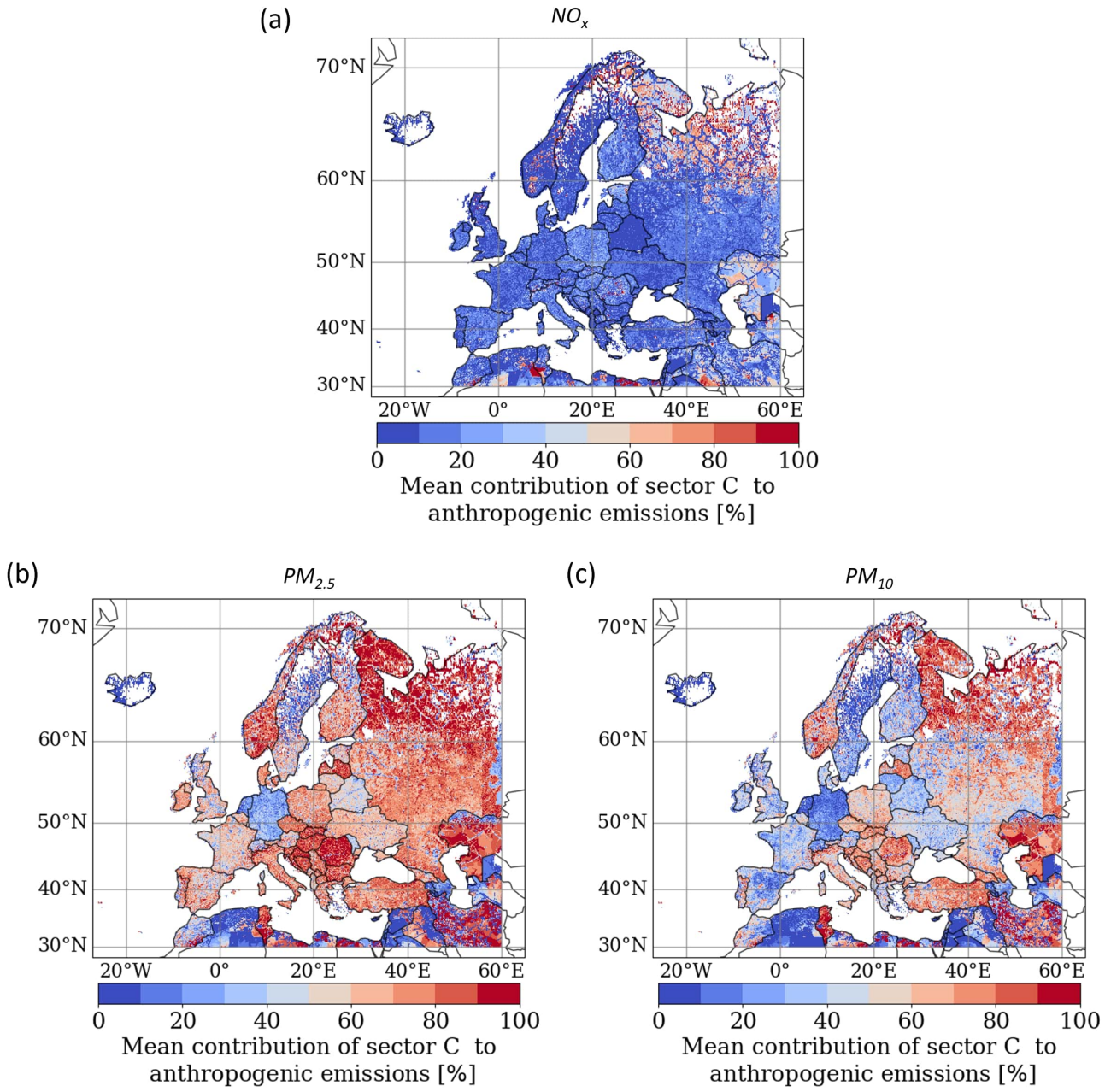

Figure S3. Spatial distribution of the average contribution of GNFR sector "Other stationary combustions" (C) to total anthropogenic emissions for NO_x (a), $PM_{2.5}$ (b) and PM_{10} (c) species over the period 2009-2018, based on the CAMS-REG-AP-v5.1 inventory (Kuenen et al., 2022).

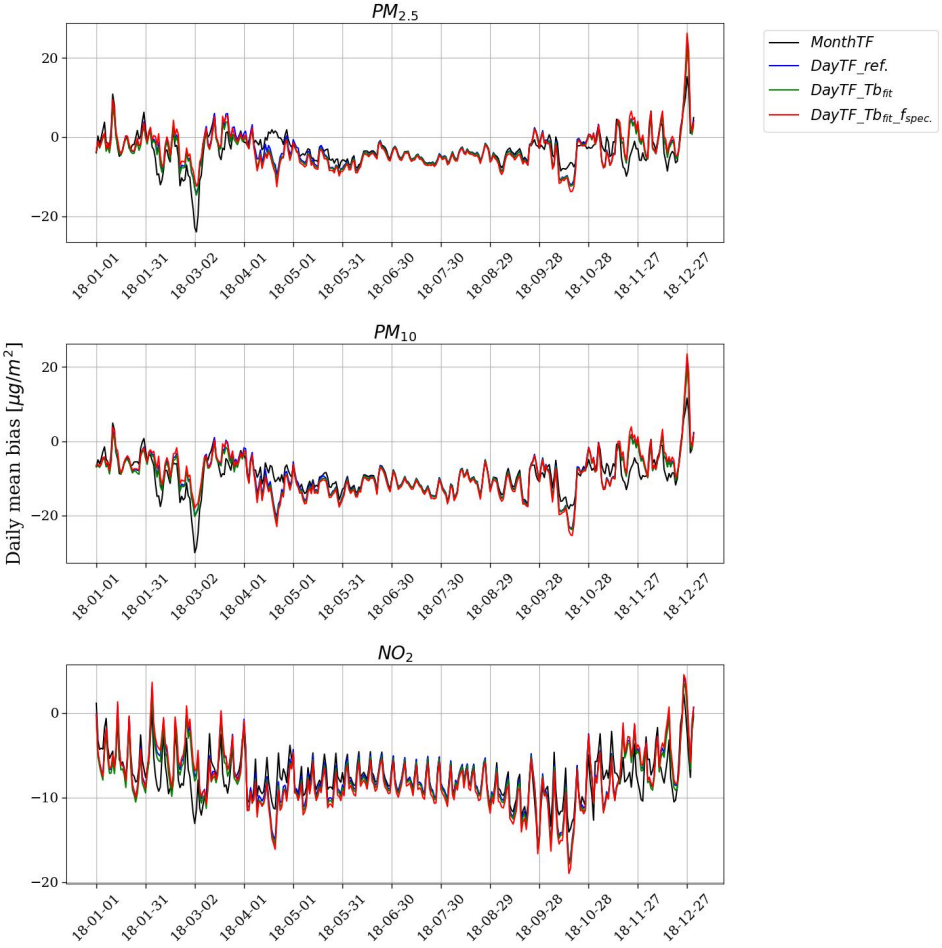

Figure S4. Evolution in 2018 of the daily average bias [$\mu g/m^3$] over the European domain between the CHIMERE simulations and the AQ e-Reporting observation stations of $PM_{2.5}$ (a), PM_{10} (b) and NO_2 (c).

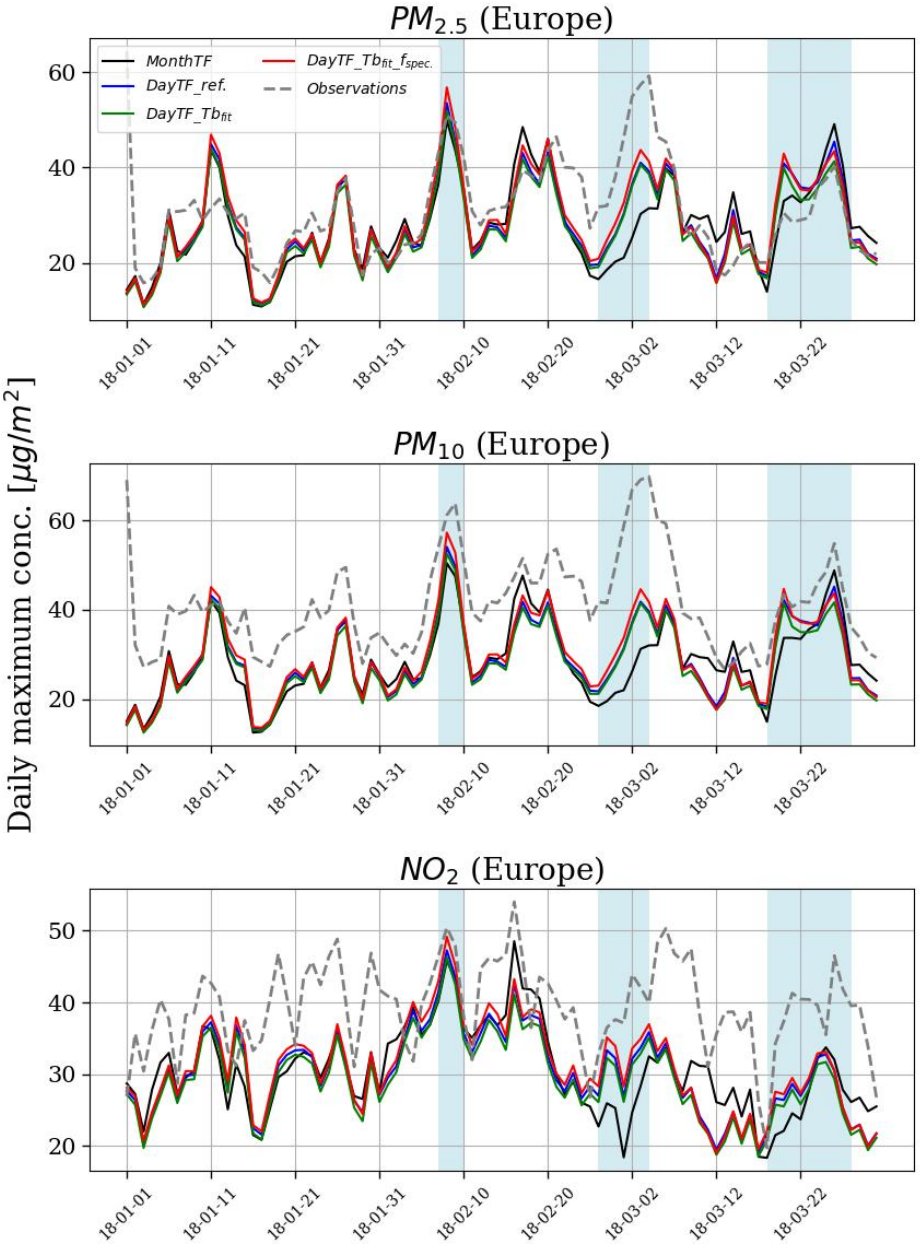

Figure S5. Daily maximum concentrations of $PM_{2.5}$ (top), PM_{10} (middle) and NO_2 (bottom) in Europe between January and March from observations (AQ-eReporting) and different CHIMERE experiments. The blue areas indicate periods of intense cold as signaled by the Climate Copernicus service.

.

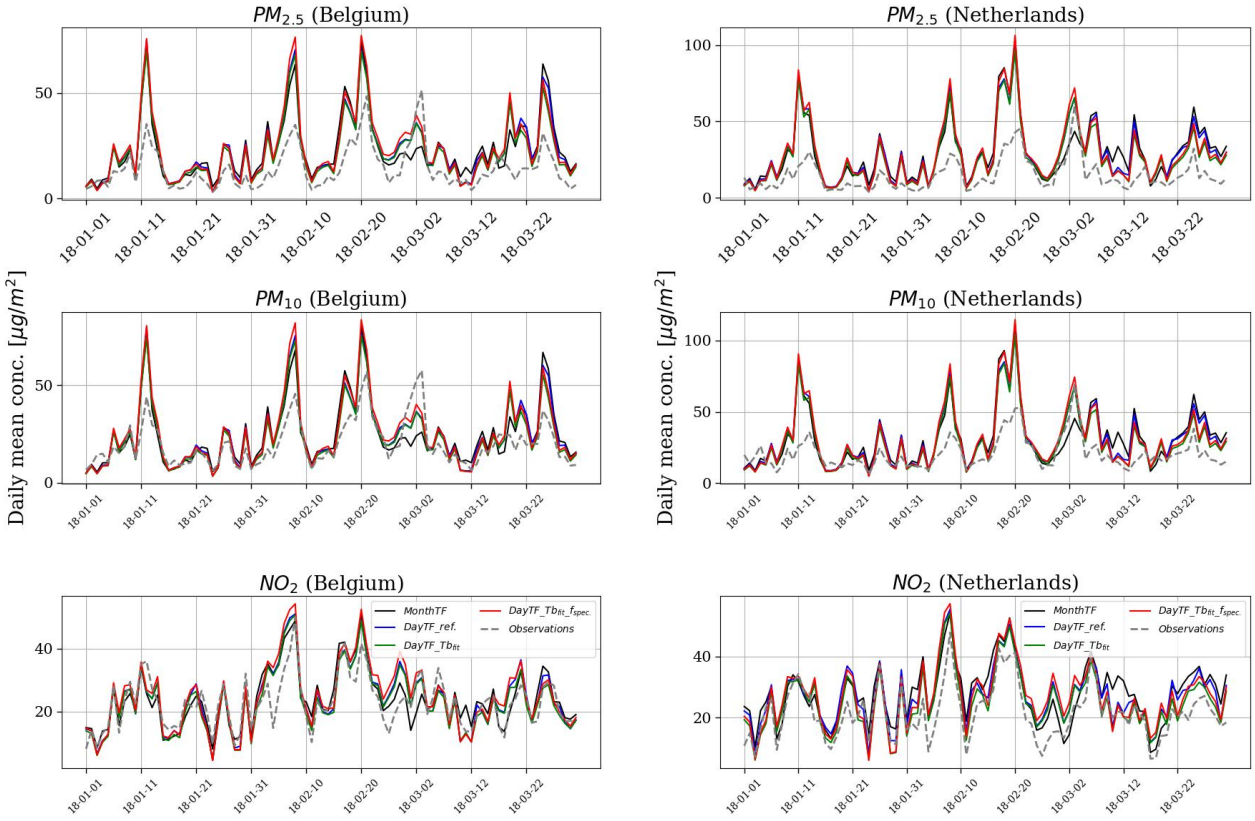

Figure S6. Average daily concentrations of $PM_{2.5}$ (top), PM_{10} (middle) and NO_2 (bottom) in Belgium (left) and Netherlands (right) between January and March from observations (AQ-eReporting) and different CHIMERE simulations.

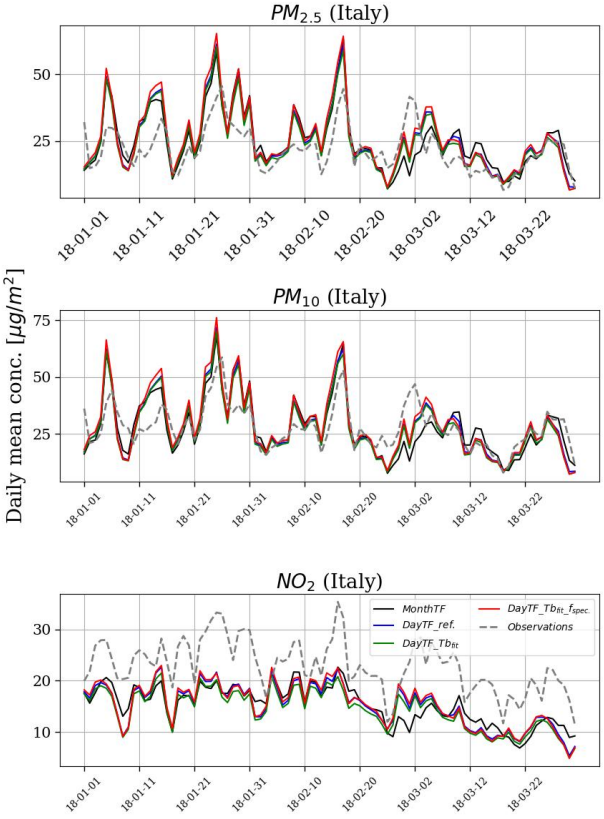

Figure S7. Same as Figure S6 for Italy.

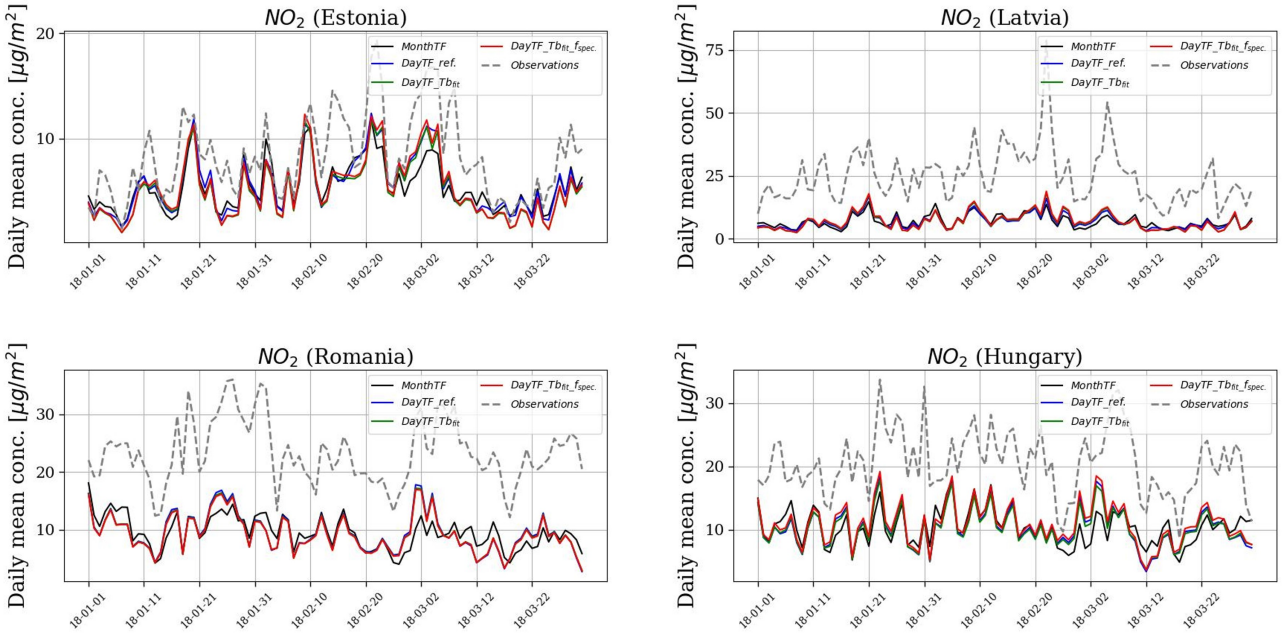

Figure S8. Average daily concentrations of NO_2 in Estonia (upper left), Latvia (upper right), Romania (lower left) and Hungary (lower right) between January and March from observations (AQ-eReporting) and different CHIMERE simulations.

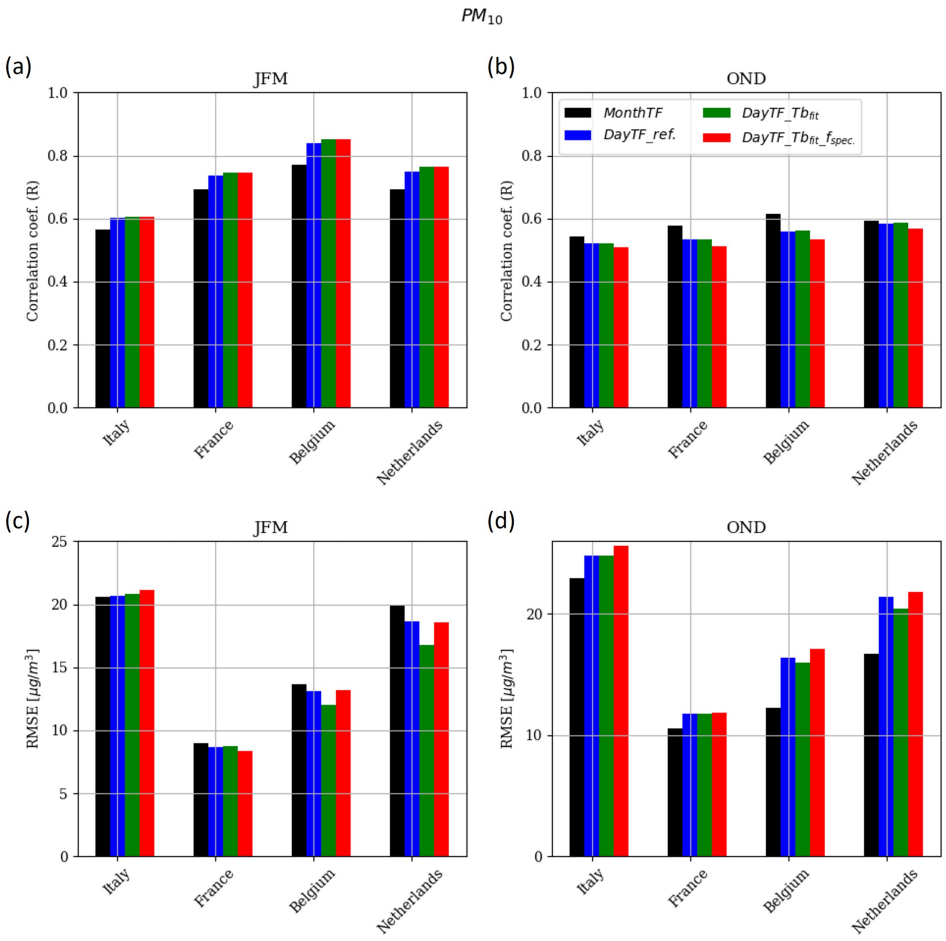

Figure S9. Spearman correlation (R coefficient) and RMSE ($\mu g/m^3$) of hourly PM_{10} concentrations for the months JFM (panel (a) and (c) respectively) and OND (panel (b) and (d) respectively), averaged over stations in countries that have been fitted with gas consumption data and for which concentration measurements are available.

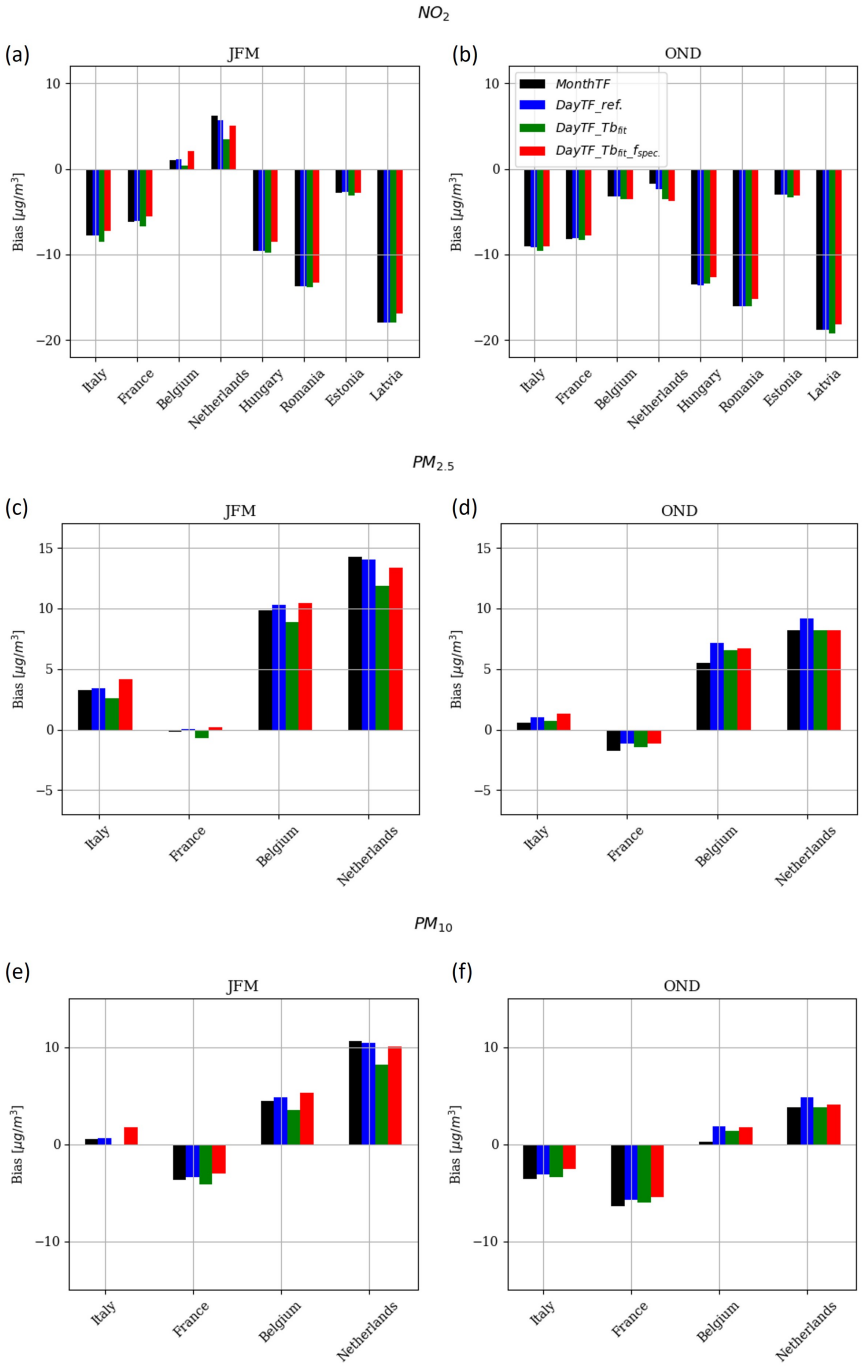

Figure S10. Average bias ($\mu g/m^3$) of hourly NO_2, $PM_{2.5}$, PM_{10} concentrations for the months JFM (panel (a), (c), (e) respectively) and OND (panel (b), (d), (f) respectively), averaged over stations in countries that have been fitted with gas consumption data and for which concentration measurements are available.

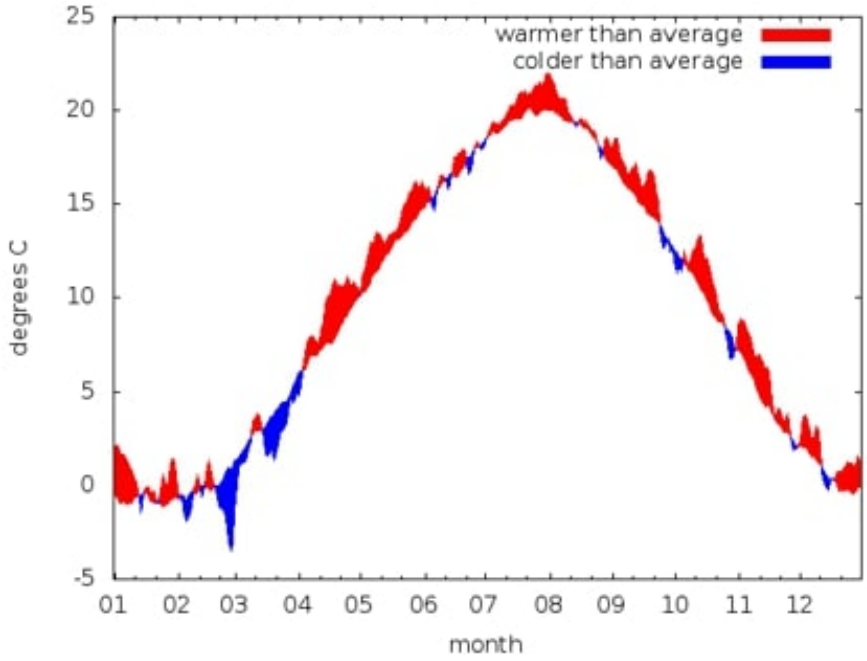

Figure S11. Daily anomalies of the European mean surface temperature for 2018, relative to 1981-2010. Data source: E-OBS, Credit: Copernicus Climate Change Service (C3S)/KNMI (https://climate.copernicus.eu/cold-start-year).

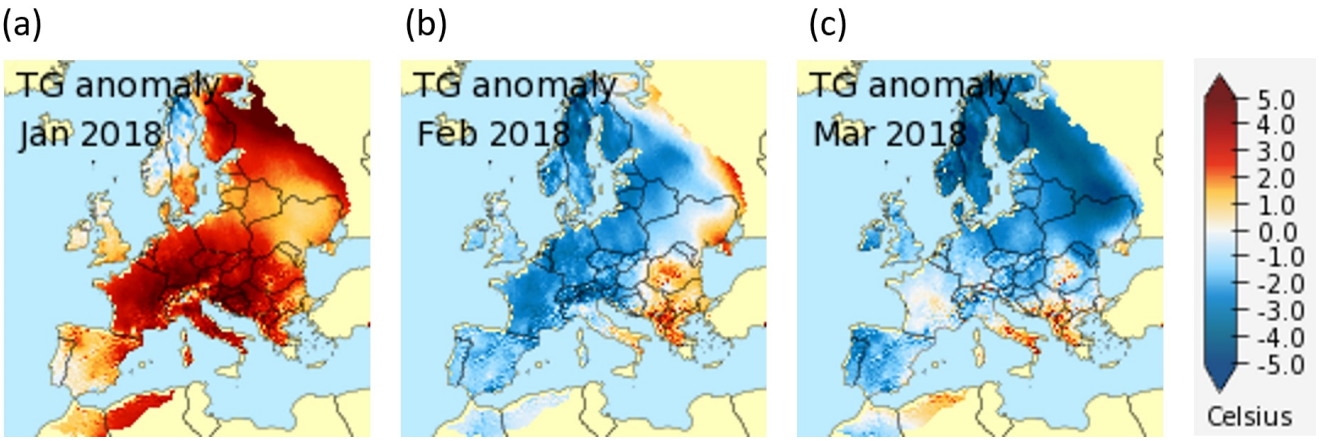

Figure S12. Differences of average temperature between January 2018 (a), February 2018 (b) and March 2018 (c), and the reference period 1981-2010. Data source: E-OBS, Credit: Copernicus Climate Change Service (C3S)/KNMI (https://surfobs.climate.copernicus.eu/stateofthecliimate/).

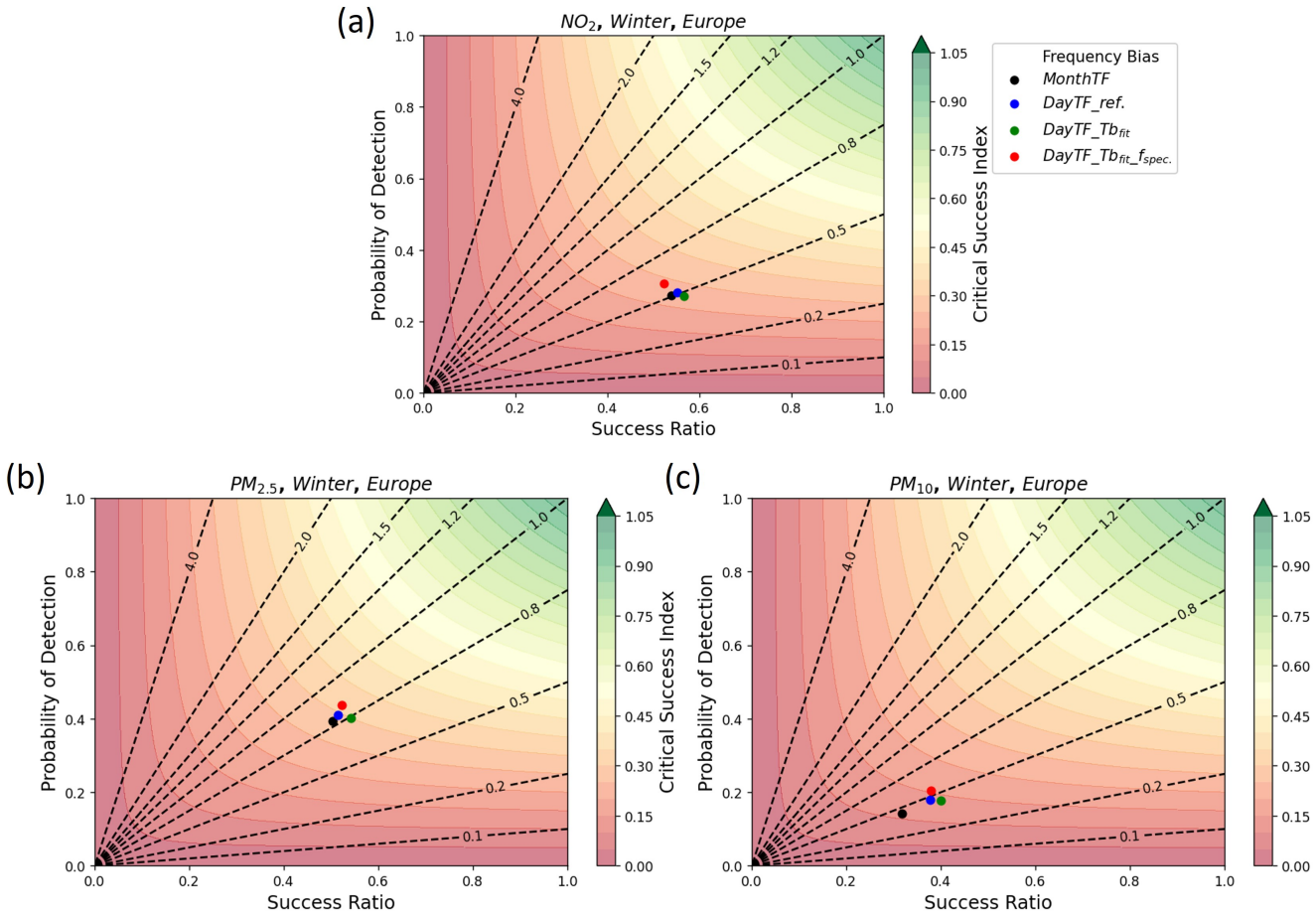

Figure S13. Performance diagram, as designed by Roebber (2009), comparing the ability to simulate the threshold exceedance (as a daily average) for the different experiments for NO_2 (a), $PM_{2.5}$ (b) and PM_{10} (c) averaged over Europe during the JFM months. The probability of detection is shown on the vertical axis, the success ratio on the horizontal axis, the frequency bias by the dashed line and the critical success index by the curved lines.

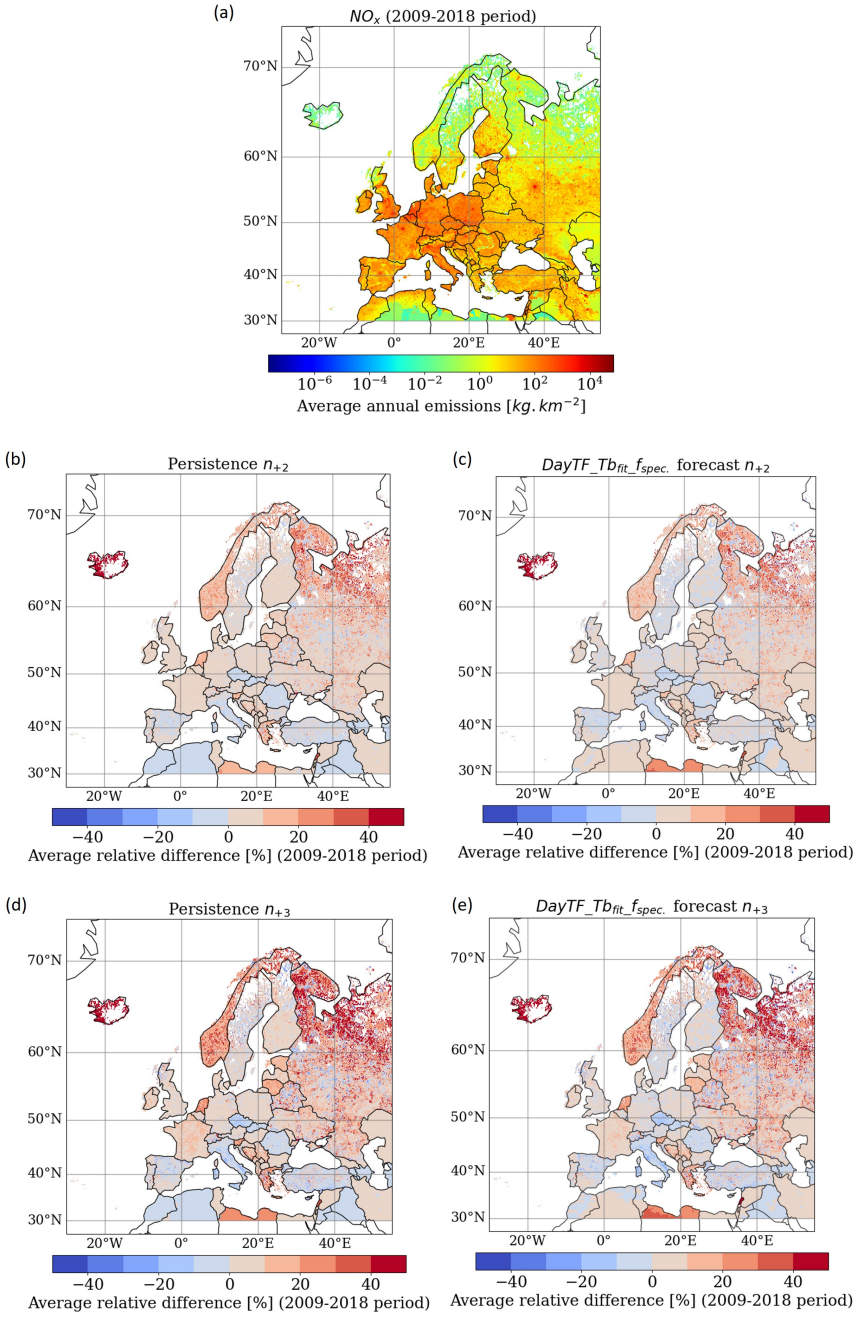

Figure S14. Spatial distribution of average annual NO_x emissions [kg/km^2] from $GNFR\_C$ (2009-2018 period), based on the CAMS-REG-AP-v5.1 inventory (a). Average relative difference using "$DayTF\_Tb_{fit}\_f_{spec.}$" to project in n_{+2} (b) in n_{+3} (d) for each year between 2009 and 2019, compared to the reported emissions. Average relative difference using the persistence method for n_{+2} (c) and n_{+3} (e) over 2009-2018.